JEM Journal of Experimental Medicine

ARTICLE

Maternally transferred mAbs protect neonatal mice from HSV-induced mortality and morbidity

Iara M. Backes[1,2], Brook K. Byrd[2], Matthew D. Slein[1,2], Chaya D. Patel[1], Sean A. Taylor[1], Callaghan R. Garland[1], Scott W. MacDonald[3], Alejandro B. Balazs[3], Scott C. Davis[2], Margaret E. Ackerman[1,2], and David A. Leib[1]

Neonatal herpes simplex virus (nHSV) infections often result in significant mortality and neurological morbidity despite antiviral drug therapy. Maternally transferred herpes simplex virus (HSV)-specific antibodies reduce the risk of clinically overt nHSV, but this observation has not been translationally applied. Using a neonatal mouse model, we tested the hypothesis that passive transfer of HSV-specific human mAbs can prevent mortality and morbidity associated with nHSV. The mAbs were expressed in vivo via vectored immunoprophylaxis or recombinantly. Through these maternally derived routes or through direct administration to pups, diverse mAbs to HSV glycoprotein D protected against neonatal HSV-1 and HSV-2 infection. Using in vivo bioluminescent imaging, both pre- and post-exposure mAb treatment significantly reduced viral load in mouse pups. Together these studies support the notion that HSV-specific mAb-based therapies could prevent or improve HSV infection outcomes in neonates.

Introduction

Among perinatal viral infections, neonatal herpes simplex virus (nHSV) infection has the highest infant mortality rate (Williams et al., 2013; Slutsker and Schillinger, 2021). Transmission most often occurs during birth or via close contact with an infected individual in the first few days of life (Brown et al., 1997). It is estimated that there are 14,000 cases of nHSV per year globally (Looker et al., 2017), and recent studies suggest rising incidence in the United States (Mahant et al., 2019). nHSV presents clinically in three forms: skin, eye, and mouth; central nervous system (CNS); and disseminated disease in the visceral organs. Despite aggressive antiviral treatment with acyclovir, mortality subsequent to disseminated disease remains high (30%), and CNS disease is associated with ∼70% neurological morbidity and 25% mortality (Whitley et al., 1991; Brown et al., 1997; Corey and Wald, 2009). This disease burden highlights the urgent need to augment clinical interventions in nHSV infections.

Maternal infection and seropositivity can reduce the risk of nHSV acquisition. The greatest risk (30–50%) is to vaginally delivered neonates born to seronegative mothers with primary or first-time genital infection (Brown et al., 1991; Brown et al., 1997; Corey and Wald, 2009; Whitley et al., 1980; Brown et al., 1991). In contrast, the risk of infection resulting from reactivated genital HSV disease is ∼3%. This suggests that maternal seroconversion and subsequent placental and/or milk transfer of antibodies (Abs) protect the neonate from HSV infection (Whitley et al., 1980; Kohl et al., 1989; Brown et al., 1991, 2003; Corey and Wald, 2009). Supporting these clinical observations, maternal seropositivity induced by vaccination, infection, or passive transfer of polyclonal HSV-specific IgG during pregnancy reduced the risk of mortality and/or neurological morbidity in mouse pups (Patel et al., 2019; Patel, 2020).

Several HSV-specific monoclonal antibodies (mAbs) targeting envelope glycoproteins prevent ocular (Wang et al., 2017), genital (Krawczyk et al., 2013; Sanna et al., 1996), and systemic HSV disease in adult mouse models (Lai et al., 2010; Lai and Chan, 2013). Given the high susceptibility of neonatal mice to HSV infection, it is of interest to investigate whether mAbs that show efficacy in adult mice also prevent disease in neonatal mice. In agreement with adult mouse studies, protection in newborn mice depends on epitope specificity, with the protection afforded by select mAbs or polyclonal antigen-specific Ab preparations (Kohl et al., 1990). Here, we evaluated a set of four human IgG1 mAbs that target the viral entry mediator glycoprotein D (gD; Wang et al., 2017; Lee et al., 2013; Clementi et al., 2016; Burioni et al., 1994). gD is present on HSV-1 and HSV-2 envelopes as well as the surface of infected cells (Stannard et al., 1987). Clinical trials of subunit vaccines that included gD in their preparation did not meet end-point efficacy (Corey et al., 1999;

[1]Department of Microbiology and Immunology, Geisel School of Medicine at Dartmouth, Lebanon, NH; [2]Thayer School of Engineering, Dartmouth College, Hanover, NH; [3]Ragon Institute of MGH, MIT and Harvard, Cambridge, MA.

Correspondence to Margaret E. Ackerman: margaret.e.ackerman@dartmouth.edu; David A. Leib: david.a.leib@dartmouth.edu.

Belshe et al., 2012) in part because the vaccinees were unable to generate substantial Abs to key gD epitopes (Hook et al., 2018). This significant pitfall could be circumvented by the use of prescreened mAbs with defined specificity. Indeed, two of the three mAbs being evaluated in current clinical trials use gD as a target, prompting us to include mAb E317/UB-621 (NCT02346760, NCT03595995, NCT04714060, and NCT04979975) and HSV8 in this study (NCT02579083). To increase the breadth of gD coverage, we also included mAbs CH42 and CH43, which have been recently evaluated in adult mice (Wang et al., 2017). Thus, these four gD-specific mAbs were evaluated for their potential to prevent HSV mortality and disseminated disease in a neonatal mouse infection model.

Given the evidence that polyclonal maternal antibodies are naturally protective against nHSV, we hypothesized that maternally transferred mAbs could have therapeutic utility. To address this, dams were given an injection of recombinant mAbs or adeno-associated virus (AAV)-vectored antibody delivery (Balazs et al., 2012), a strategy that can protect adult animals from viral (Balazs et al., 2013; Balazs et al., 2014; Jong et al., 2014) and parasitic infections (Deal et al., 2014), but which has not been evaluated for its ability to provide transgenerational protection in the form of maternally transferred Abs. Together our work demonstrates that maternal or direct administration of mAbs can ameliorate or prevent this devastating neonatal disease, motivating clinical investigation.

Results

mAb UB-621 accumulates at the placental–fetal interface

The mAbs used in this study span the gD ectodomain, with epitopes close to the herpes virus entry mediator (HVEM) binding domain, and the Nectin (1 and 2) binding domains (Fig. 1 A). The gD:mAb interfaces between E317/UB-621, CH42, and CH43 have been resolved in detail through crystallography and alanine scanning (Wang et al., 2017; Lee et al., 2013), while that of HSV8 is more broadly defined from binding experiments with truncated gD (De Logu et al., 1998; Fig. 2 B). Each of these mAbs protects from HSV infection in adult mouse models (Table S1), and two (E317/UB-621 and HSV8) are currently in clinical trials (E317/UB-621: NCT02346760, NCT03595995, NCT04714060, and NCT04979975; HSV8: NCT02579083).

While maternal Abs prevent nHSV mortality and morbidity (Jiang et al., 2017; Patel et al., 2019), their biodistribution in pregnant dams has not been fully elucidated. To preserve the complex anatomy of the placental–fetal interface, we pursued hyperspectral imaging via whole body cryo-macrotome processing (Soter et al., 2020), which causes minimal disruption to these tissues (Fig. 2). We administered fluorescently labeled UB-621 mAb to pregnant C57BL6 (B6) dams 2 d before sacrifice and tissue preparation. Two dams (naive and UB-621 infused) were immediately processed for cryo-imaging after sacrifice, while an additional dam was further dissected to prepare conceptuses for cryo-imaging. A robust fluorescent signal of tissues at the placental–fetal interface was detected in the cryo-imaged dam infused with fluorescent UB-621 as compared with the control dam that did not receive mAb (Fig. 2, A and B; and Video 1). To confirm that this signal originated from tissues at the maternal–fetal interface, conceptuses were individually harvested from the maternal uterus and individually imaged with different layers of placental–fetal and/or fetal tissues dissected (Fig. 2 C). These dissection experiments confirmed that mAb accumulated at the placental–fetal interface and was also detected in fetal and maternal tissues (Fig. S1). When assessing fetal tissues, greater variability was observed with dissected tissues, potentially reflecting the different maternal and fetal layers that were differentially exposed prior to cryopreservation. Notably, high fluorescence was observed in a harvested conceptus where the visceral yolk sac, a tissue rich in the expression of the neonatal Fc receptor (FcRn) necessary for IgG transfer (Kim et al., 2009), remained intact (Fig. 2 C, middle image). Overall, this technique allowed us to visualize IgG traversing the circulation of the pregnant dam and entering maternal and fetal membranes.

HSV mAbs targeting gD protect neonatal mice from HSV-1 and HSV-2 mortality

Like human neonates, mouse pups are highly susceptible to HSV infection, succumbing to infection at low viral doses relative to adult mice (Zawatzky et al., 1982; Kohl and Loo, 1980). Therefore, we wished to determine if HSV gD-specific mAbs could protect mouse pups from HSV-1 infection. Pregnant dams were administered either CH42 or control IgG ∼3–5 d before parturition, and the pups were challenged intranasally with HSV-1 1 d after birth (Fig. 3 A). The offspring of dams treated with CH42 showed significantly improved survival ($P < 0.001$) compared with offspring of control IgG-treated dams.

While prophylactic approaches for nHSV are desirable, we also sought to model therapeutic approaches to treat extant infections in neonates that may more closely model the clinical setting. To understand the prophylactic and therapeutic effect of mAb treatment, we administered E317 or control mAb (both at ∼6.45 mg/kg) 1 d before viral challenge. Given results with prophylactic maternal CH42 treatment, we administered CH42 or control mAb (both at ∼25 mg/kg) 1 d after viral challenge. Pups treated with E317 or CH42 exhibited improved survival ($P = 0.06$ and $P < 0.05$, respectively) relative to pups that received control IgG (Fig. 3 B). Notably, when used prophylactically, E317 (∼6.45 mg/kg) protected all mouse pups from lethal infection.

We next assessed the protection afforded by mAbs currently being evaluated in clinical trials for adult genital HSV disease (HSV8 and UB-621; Clementi et al., 2016; Politch et al., 2021; E317/UB-621: NCT02346760, NCT03595995, NCT04714060, and NCT04979975; HSV8: NCT02579083). HSV8, UB-621, CH42, or control IgG were administered to pups and then mice were immediately challenged with HSV-1. Both HSV8 and UB-621 mAbs completely protected pups from mortality following HSV-1 viral challenge ($P < 0.001$). In contrast, CH42 afforded partial protection compared with control IgG-treated pups ($P < 0.01$; Fig. 3 C, left panel).

While HSV-1 genital disease predominates in the Americas and Western Pacific and continues to rise as the etiologic agent of genital disease in high-income countries, HSV-2 remains a significant cause of neonatal disease. Therefore, pups were

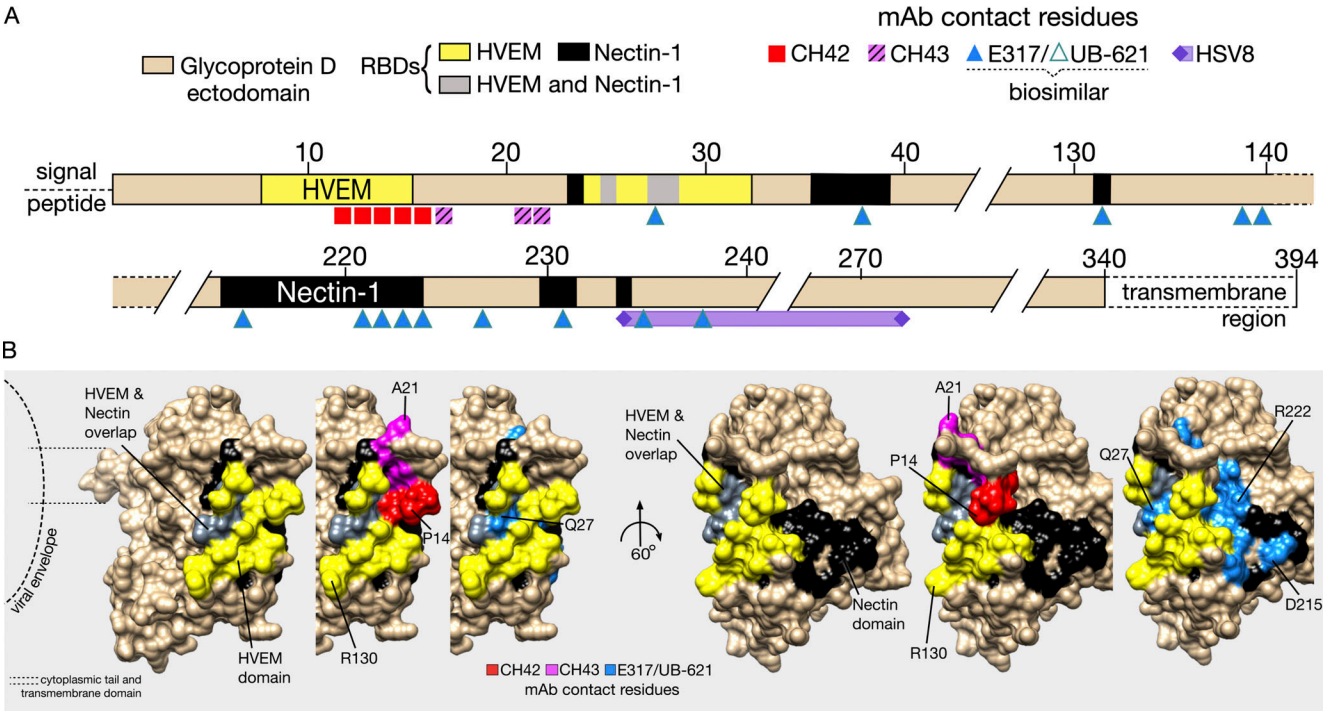

Figure 1. **Epitope map of HSV-specific mAbs that target the viral entry mediator gD. (A)** Linear representation of the gD extracellular domain with the HVEM binding domain (yellow) and Nectin domains (black). UB-621 is a clinical-grade product of the E317 clone. The exact contact residues of HSV8 are not known, but shown is an approximation based on reactivity against gD residues 235–275. **(B)** The space-filling structure of truncated gD (gD285; PDB accession no. 1JMA), with cell receptor binding domains and mAb epitopes denoted by specific colors shown in A, as follows: red = CH42, pink = CH43, blue = E317/UB-621, purple = HSV8. Residues (P14, A21, Q27, R130, D215, R222) are numbered as points of reference.

treated with HSV8, UB-621, and CH42, as described above, and challenged with HSV-2 (Fig. 3 C, right panel). Each HSV-specific mAb tested resulted in significantly improved (UB-621 $P < 0.001$, CH42 and HSV8 $P < 0.01$) survival of pups challenged with HSV-2 as compared with control IgG-treated pups. Collectively, these data showed that gD-specific mAbs can protect highly susceptible neonatal mice when administered via disparate routes, at different doses of the antibody, and before and after viral challenge with either HSV-1 or HSV-2.

mAb CH42 reduces CNS and disseminated viral replication

Disseminated disease results in the highest case fatality rate among nHSV clinical presentations, and despite aggressive antiviral treatment, has an unacceptably high mortality (30%; Corey and Wald, 2009). We, therefore, assessed the impact of mAb therapy in the control of viral dissemination using bioluminescent imaging (BLI) to monitor viral replication and spread in real-time (Fig. 4). Dams or pups received CH42 mAb or control IgG either before or after the challenge with recombinant HSV-1 that expresses luciferase (Summers et al., 2001; Luker et al., 2002). We performed BLI every other day from 2 to 8 d after infection. As expected (Patel et al., 2019; Jiang et al., 2017), the virus was detected primarily in the lungs, trigeminal ganglia, and brain (Fig. 4 and Fig. S2). Among the different treatment and timing modalities tested, offspring of mAb-treated dams cleared the infections fastest compared with control IgG ($P < 0.001$), with nearly undetectable bioluminescence even at the earliest time point assessed (Fig. 4, A and D). When antibody and virus were administered simultaneously, or when the antibody was administered 1 d following infection, a similar pattern was apparent: bioluminescence diminished more rapidly in CH42- rather than control IgG-treated pups over time and reached background levels by day 6 (Fig. 4, B, C, E, and F). While mAb prophylaxis of the pregnant dam resulted in the best viral suppression, co- and postinfection mAb treatment also conferred protection, demonstrating the efficacy of mAb therapy for nHSV.

HSV-specific mAbs delivered via vectored immunoprophylaxis (VIP) provide transgenerational protection from nHSV mortality

Having shown that administration of mAbs to dams protects their pups from nHSV mortality, we sought to investigate VIP using AAV-mediated Ab delivery. HSV-specific in vivo AAV-expressed mAbs (CH42, CH43, and E317) and one control IgG mAb (IgG_1 targeting human immunodeficiency virus envelope glycoprotein) were used in these studies. Female mice received a single intramuscular injection of a nonintegrating AAV8 encoding a human mAb (Fig. 5 A). Serum was obtained over a 4-wk period to confirm mAb expression (Fig. 5 B). Progeny of AAV-transduced dams had detectable levels of mAbs in the serum (Fig. 5 C and Fig. S3 A). Furthermore, mAb was effectively transferred throughout visceral organs and the nervous system (Fig. 5 C). Antibody biodistribution was similar to that observed in neonatal mice that received direct intraperitoneally (i.p.) injected mAb (Fig. S3 B). The notable exception was that pups born

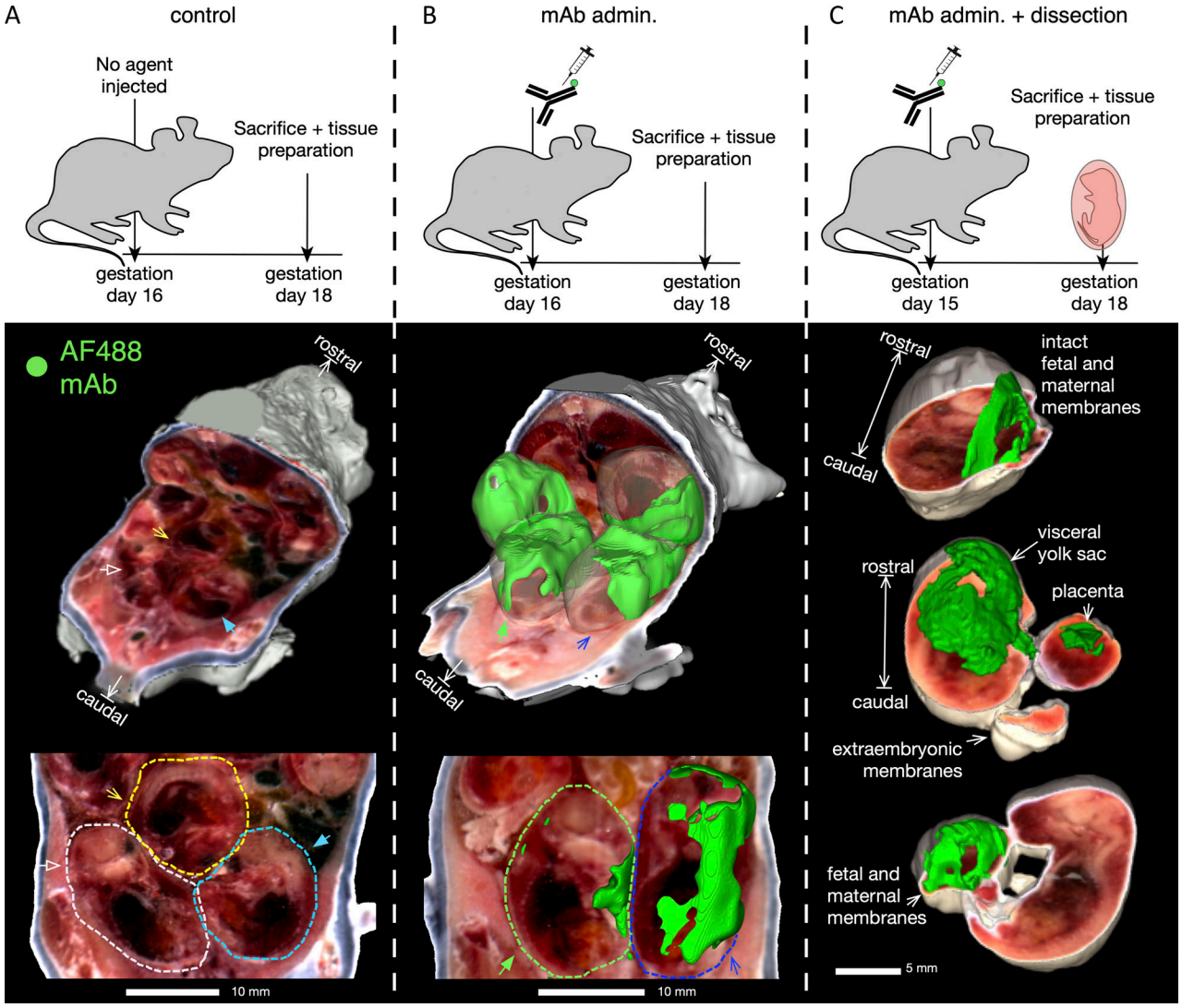

Figure 2. **Fluorescently labeled mAb accumulates at the placental–fetal interface.** To assess maternally administered Ab biodistribution, conjugated Ab was administered intravenously (IV) on day 15 or 16 of gestation to B6 mice, then 2–3 d later tissues were prepared for whole body imaging using the cryo-macrotome. **(A)** Background fluorescence levels in a pregnant dam (n = 1) not injected with conjugated Ab. **(B)** Accumulation of fluorescently labeled UB-621 Ab in a pregnant dam (n = 1) 2 d following IV administration. **(C)** Accumulation of fluorescently labeled Ab following administration to the pregnant dam (n = 1) in a subset (showing 3 of 6 pups) of harvested conceptuses from the murine uterus, with maternal and fetal layers removed as indicated.

to AAV-transduced dams had higher mAb signal originating from the stomach, indicative of mAbs present in ingested breastmilk.

Finally, to assess whether the transferred mAbs were sufficient to protect pups from a lethal viral challenge, progeny of AAV-transduced dams were challenged with HSV-1 2 d postpartum and monitored until weaning at 3 wk of age. Despite variation in the levels of transferred mAb, the progeny of HSV mAb AAV-transduced dams were completely protected from mortality, while progeny of control IgG AAV-transduced dams rapidly succumbed to infection (Fig. 5 D). These findings demonstrate that antibodies produced in vivo in dams via VIP and subsequently transferred to pups were protective ($P < 0.001$). Moreover, although pups from E317 AAV-transduced dams received considerably less mAb, they were equally protected from disease as pups that received 10–50-fold higher levels of mAbs from their mothers. These differences in expression could be attributed to variance in RNA stability, translational efficiency, protein secretion efficiency, and clearance of the circulating mAb. Transduction of dams resulted in the transfer of huIgG that was persistent enough to protect mouse pups born in their third breeding cycle, ∼6 mo after transduction, consistent with long-term expression achieved previously (Balazs et al., 2012; Balazs et al., 2013; Deal et al., 2014). Together, these findings further underscore the promise of diverse mAb delivery strategies in protection against nHSV-induced morbidity and mortality.

Discussion

A great deal of evidence supports the hypothesis that Abs protect humans and mice against nHSV (Yeager et al., 1981; Kohl et al., 1990; Brown et al., 1991, 2003; Kohl, 1991; Evans and Jones, 2002;

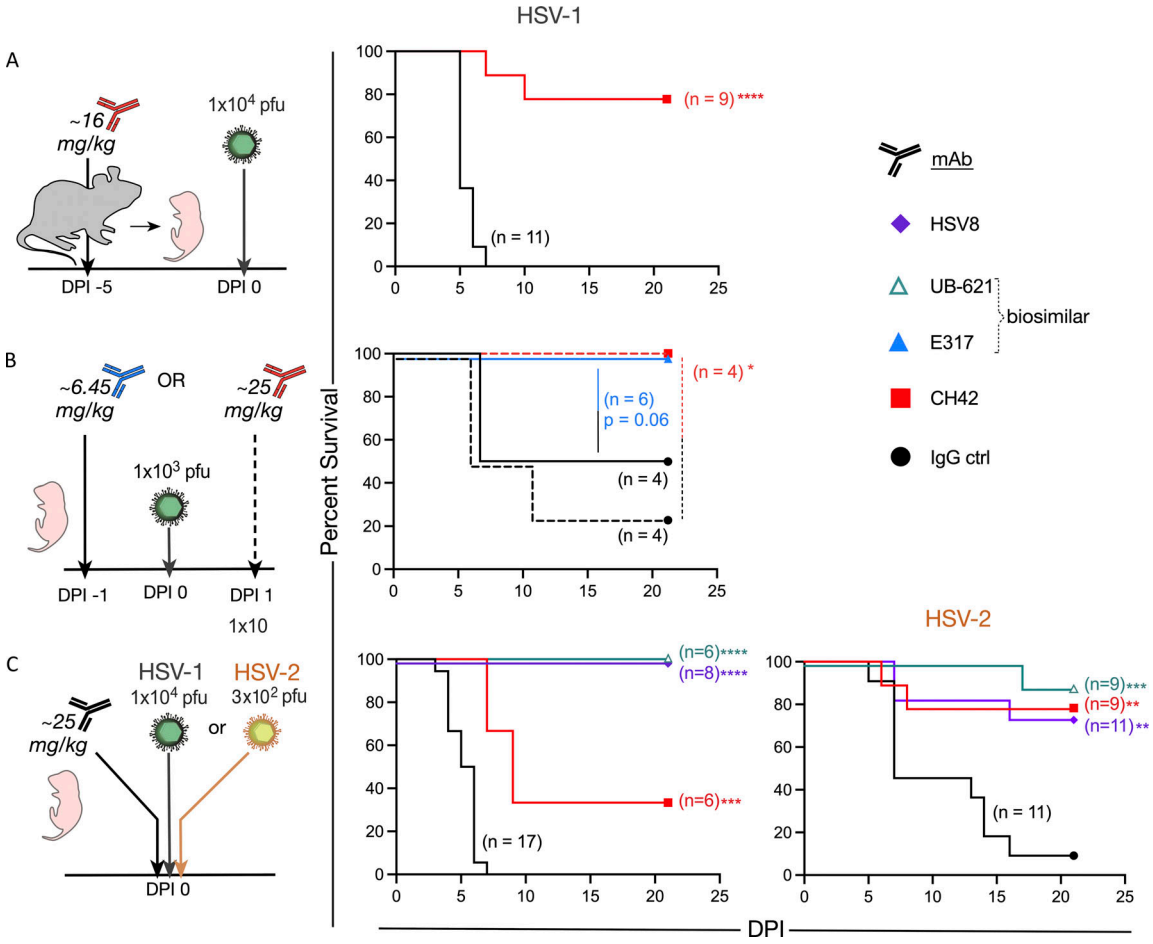

Figure 3. **Prophylactic and therapeutic HSV-specific mAbs prevent nHSV-associated mortality.** Abs were delivered intraperitonially to pregnant dams, or pups. Pups were challenged intranasally 2 d post-partum with indicated viral dose, then observed to DPI 21. **(A)** Survival of pups following administration of CH42 (red, *dam n* = 2, two litters, *pup n* = 9) or IgG control (ctrl, black, *dam n* = 2, two litters, *pup n* = 11) to B6 background pregnant dams 5 d before infection. **(B)** Survival of B6 pups following administration of E317 (blue, one litter, *n* = 6) or IgG control (black, one litter, *n* = 4) 1 d before infection in solid lines. Survival of a single litter for which one half received CH42 (red, *n* = 4) and the other half IgG control (black, *n* = 4) 1 d postinfection in dashed lines. **(C)** Survival of pups following HSV8 (purple, one litter, *n* = 8), UB-621 (teal, one litter, *n* = 6), CH42 (red, one litter, *n* = 6), or IgG control (black, two litters, *n* = 17) administration immediately before infection with HSV-1. Survival of pups following HSV8 (purple, two litters, *n* = 11), UB-621 (teal, one litter, *n* = 9), CH42 (red, one litter, *n* = 9), or IgG control (black, two litters, *n* = 11) administration immediately before infection with HSV-2. Statistical significance was determined by the Log-rank (Mantel-Cox) test; HSV-specific mAbs are compared to IgG control (ctrl). *, P < 0.05; **, P < 0.01; ***, P < 0.001. DPI, day postinfection.

Jiang et al., 2017; Patel et al., 2019, 2020; Kao et al., 2020). Several mAbs, some used in this study, ameliorate acute HSV infection in adult animal models (Wang et al., 2017; Krawczyk et al., 2013; Sanna et al., 1996; Kohl et al., 1990; Kimberlin, 2007). Despite this evidence, however, little progress has been made toward Ab-based therapies to treat nHSV in the clinic, and prior trials have relied upon acyclovir and its derivatives. Our experiments demonstrated that diverse mAbs targeting gD protect neonatal mice from lethal viral challenge and reduce virally derived bioluminescence in the viscera, peripheral nervous system (PNS), and CNS. Among mAbs tested, HSV8 (Politch et al., 2021) and UB-621 (Clementi et al., 2016) are currently being evaluated for prevention and/or reduction of adult HSV genital disease (clinical trial identifiers NCT02579083, NCT04714060, and NCT04165122). In light of our results, these mAbs should be considered for the prevention or amelioration of HSV in susceptible neonates.

Clinically, early therapeutic intervention is critical in the setting of nHSV, and delayed acyclovir treatment is associated with increased in-hospital death and morbidity (Shah et al., 2011). Likewise, our results underscore the importance of early intervention in the setting of mAb-based treatment. Among clinical presentations, disseminated disease has the highest mortality and CNS disease has the highest morbidity (Whitley et al., 1991). The use of the intranasal route of infection, which often results in viral dissemination (Patel et al., 2019; Kao et al., 2019; Jiang et al., 2017), allowed us to discern if mAbs could reduce viral load in multiple tissues. Maternal mAb administration, either by direct infusion of Ab or through VIP, gave near-complete protection to pups from nHSV. Maternal mAb administration results in the transfer of mAbs through the placenta and breast milk, which in the case of AAV-derived mAbs was observed over multiple pregnancies. This durability is consistent with the protection sustained with active maternal

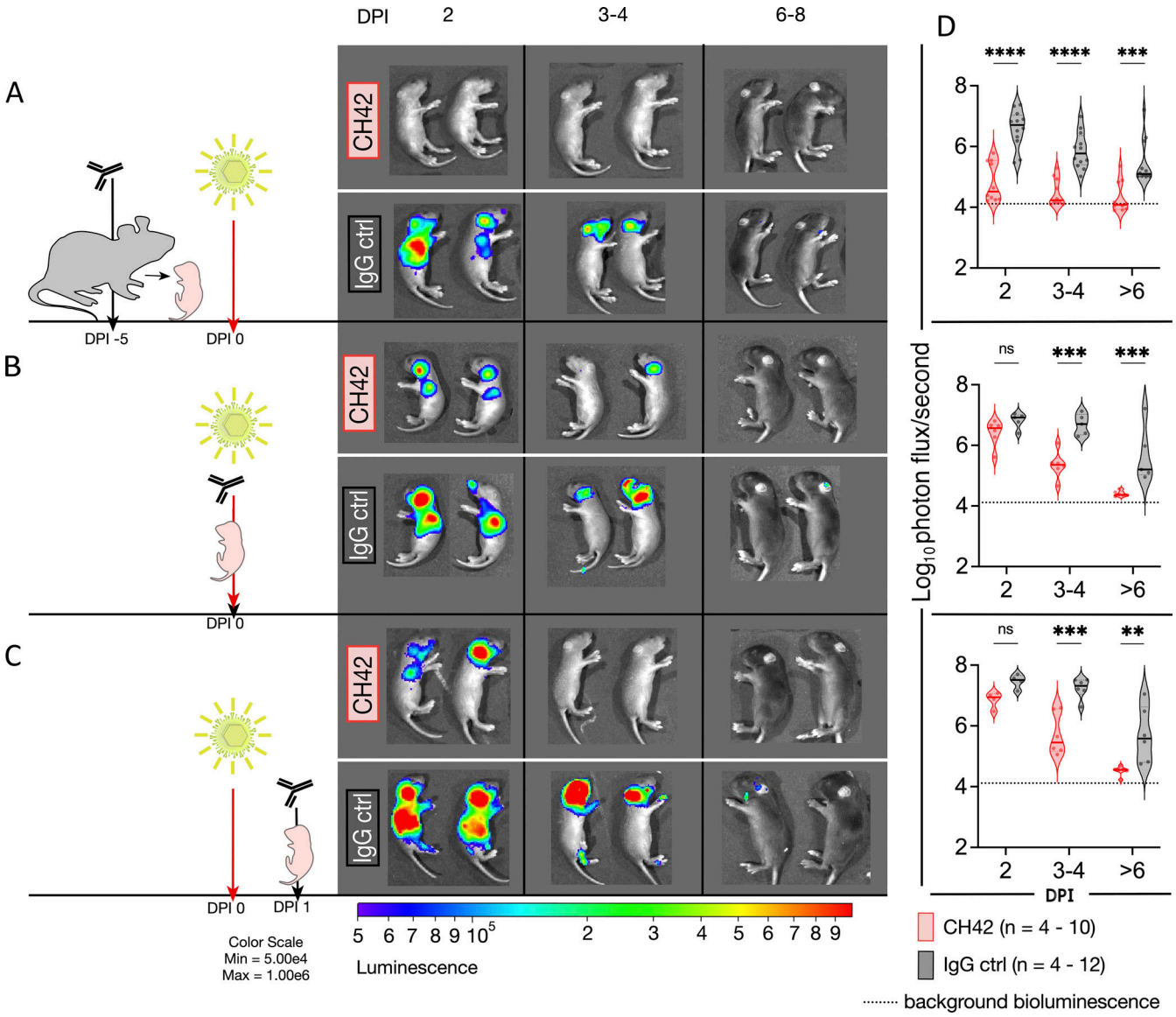

Figure 4. **Administration of CH42 reduces viral dissemination.** Pregnant dams or 2-d-old pups received intraperitoneal injections of CH42 or IgG control (ctrl) antibody before or after intranasal viral challenge with a luciferase-expressing reporter HSV-1 (1×10^5 PFU). Pups were imaged on DPI 2, then imaged until DPI 8. Representative images follow the same two pups sequentially. **(A)** Bioluminescence imaging of pups following CH42 (dam $n = 2$, two litters, pup $n = 10$) or IgG control (dam $n = 2$, two litters, pup $n = 12$) administration to pregnant dams 5 d before infection. **(B)** Bioluminescence imaging of pups following i.p. mAb administration of CH42 (dam $n = 1$, one litter, pup $n = 6$) or IgG control (dam $n = 1$, one litter, pup $n = 5$) and immediate subsequent viral challenge. **(C)** Bioluminescence imaging of pups following i.p. mAb administration of CH42 (dam $n = 2$, two litters pup $n = 4–6$) or IgG control (dam $n = 2$, pup $n = 4–6$) 1 d after infection. **(D)** The quantification of the virally derived bioluminescence in A–C in the top, middle, and bottom panels, respectively. Each dot represents an animal, the solid line is the median, and the dotted lines are the quartiles. Statistical significance was determined by two-way ANOVA, and Šídák's method for multiple comparisons (**, $P < 0.01$; ***, $P < 0.001$; ****, $P < 0.0001$). DPI, days post infection.

vaccination, also achieved over multiple pregnancies (Patel et al., 2019; Patel et al., 2020). Maternally derived mAbs were both systemically and mucosally distributed, which may explain the superior protection relative to direct pup administration. Furthermore, the progeny of AAV-transduced dams would have continually transferred mAbs throughout gestation, which not only lengthens the time to accumulation but also exposes the fetus to Abs much earlier in their development. It is not completely understood if this would have significant consequences in the clearance or biodistribution of transferred Abs when compared to Ab exposure taking place later in gestation. However, the resulting in utero accumulation of mAbs, supplemented through nursing, could provide an explanation for the excellent protection afforded by this strategy. These results are also consistent with the idea that early prophylactic treatment provides optimum protection.

Different mAbs resulted in variable protection when directly administered to pups. These differences may be attributed to distinct mechanisms of action (e.g., neutralization, antibody-dependent cellular cytotoxicity, or other effector functions),

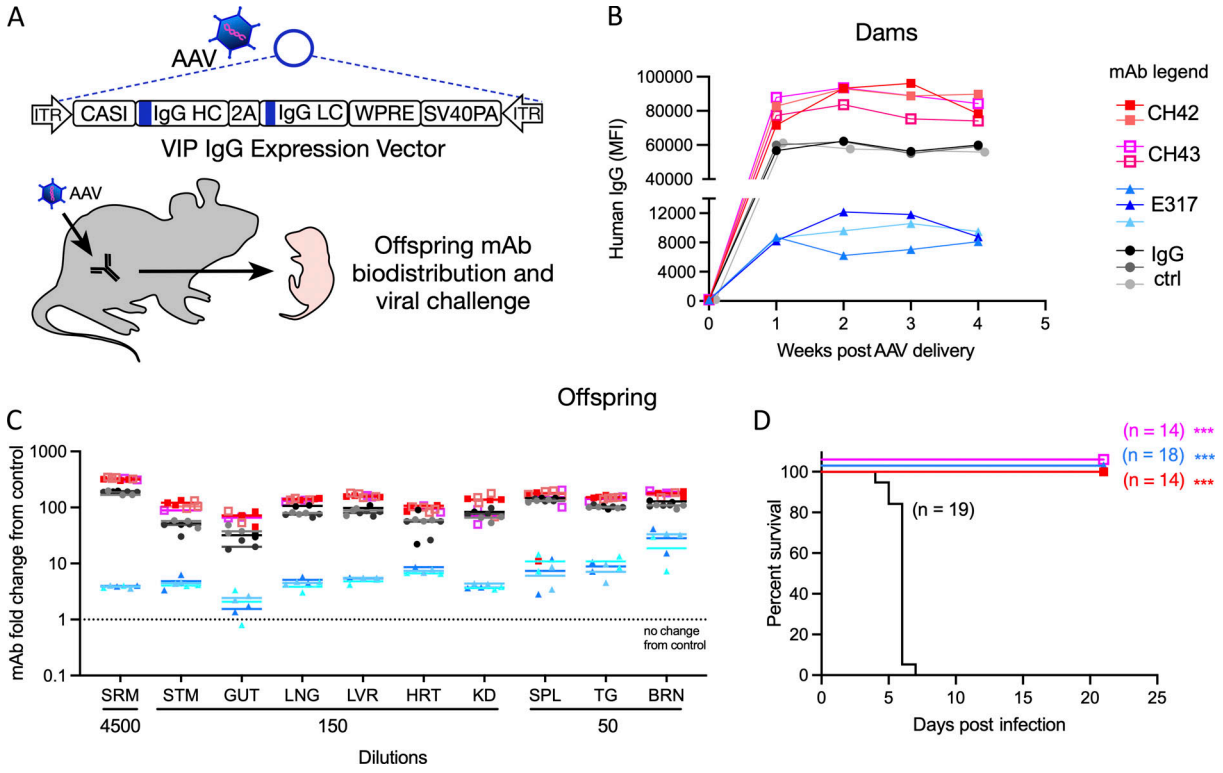

Figure 5. **AAV-derived HSV-specific transferred mAbs protect pups from nHSV mortality.** AAVs encoding four different mAb sequences were administered to female mice. Progeny were assessed for Ab transfer and protection from viral challenge. **(A)** Schematic of AAV human IgG expression vector structure and experimental approach. **(B)** Detection of in vivo expressed huIgG in the serum of AAV-administered female mice from two different litters, week 0 through 4, CH42 (n = 2), CH43 (n = 2), E317 (n = 3), and IgG ctrl (n = 3). **(C)** Biodistribution of human IgG in the viscera, brain, trigeminal ganglia, and serum of offspring of AAV-treated dams, each symbol represents a pup, CH42 (dam n = 2, two litters, pup n = 4), CH43 (dam n = 1, one litter, pup n = 3), E317 (dam n = 3, three litters, pup n = 6), IgG ctrl (dam n = 3, three litters, pup n = 8), the bars represent geometric mean. Signal is reported as the fold increase in human IgG in treated pups relative to untreated controls. **(D)** Survival of progeny of AAV-administered dams challenged with 1×10^4 PFU of HSV-1 2 d post-partum, CH42 (dam n = 2, two litters, pup n = 14), CH43 (dam n = 2, two litters, pup n = 14), E317 (dam n = 3, three litters, pup n = 18), IgG ctrl (dam n = 3, three litters, pup n = 19). Statistical significance was determined by the Log-rank (Mantel-Cox) test; HSV-specific mAbs are compared to IgG control (ctrl; ***, $P < 0.001$). Serum (SRM), stomach (STM), lung (LNG), liver (LVR), heart (HRT), kidney (KD), spleen (SPL), trigeminal ganglia (TG), brain (BRN).

and/or differences in epitope affinity or specificity. More specifically, consistent with differences in survival between HVEM and Nectin knockout mice challenged with HSV (Kopp et al., 2014; Kopp et al., 2013; Kopp et al., 2009), the differing receptor binding domains targeted by these mAbs could explain this variation. Both E317/UB-621 and HSV8 are robust neutralizers of HSV-1 and HSV-2 (Burioni et al., 1994; Lai et al., 2010), while CH42 and CH43 can only protect engineered cells lines that express HVEM alone (Wang et al., 2017). In vivo, attenuated infection has been demonstrated in mice that lack Nectin-1, indicating that it is the predominant receptor by which HSV initiates viral entry in mice. These data suggest that neutralization and effector activity may afford protection when E317/UB-621 and HSV8 are administered. In contrast, CH42 and CH43 likely rely predominantly on non-neutralizing functions.

Overall, we conclude that the mAbs tested in this study are effective and that the mode, dose, and timing of mAb administration are key determinants of protection. Prophylactic use of mAb to the respiratory syncytial virus (RSV) demonstrates the feasibility of mAb-based interventions in the neonatal and preterm population, with similar pharmacokinetics as those seen in adults (Subramanian et al., 1998; Sáez-Llorens et al., 1998). Recently, the half-life extended engineered mAb, VRC01-LS, which targets HIV, was administered to newborns and infants. These mAbs were well tolerated with minimal adverse events, and when compared to unaltered VRC01, the LS-engineered version was present at significantly higher levels at 4 and 8 wk after administration (Cunningham et al., 2020; McFarland et al., 2021). While neonates have a shorter window of vulnerability to HSV as compared with RSV and HIV, the long half-life of IgG1, which can be prolonged with mAb engineering (Zalevsky et al., 2010; Booth et al., 2018), could provide a single-dose strategy to protect from diseases. These data provide strong support to the idea that pre- and post-exposure mAb administration protects neonates from HSV infection.

Current clinical strategies to prevent nHSV involve the administration of antivirals to mothers with a history of genital herpes or, in cases of primary HSV infection, cesarean section (Brown et al., 2003; Sheffield et al., 2006). Importantly, our model uses maternal Ab therapy, which has the potential to protect both the mother and neonate. Collectively, we show that mAbs transfer to neonates and distribute to visceral organs and the nervous system. This observation is consistent with the distribution of natural maternally derived mouse and human

Abs (Patel, 2020; Jiang et al., 2017). In agreement with the hypothesis that Abs protect neural tissues from viral spread (McKendall et al., 1979; Oakes, 1975; Dix et al., 1981), we have previously shown that active maternal vaccination protected mice from neurobehavioral pathology (Patel et al., 2019; Patel et al., 2020). These results represent an exciting opportunity to pursue maternal mAb-based interventions to prevent congenital and perinatal disease in at-risk populations. There are >260 clinical trials exploring AAV-based gene delivery (Bulcha et al., 2021). In its most successful platform, AAV-mediated therapy has demonstrated clinical efficacy up to 6 yr after a single administration (Gaudet et al., 2016). Encouragingly, two clinical trials to date have explored AAV-based HIV-specific mAb delivery (PG9: NCT01937455 and VRC07: NCT03374202) with excellent safety profiles (Casazza et al., 2022; Priddy et al., 2019). AAV-expressed VRC07 was detected 3 yr after delivery in half of the study participants. While anti-drug Abs (ADA) reactive to the expressed mAbs have been reported (Casazza et al., 2022), AAV8-derived mAb expression in B6 mice has shown minimal immunogenicity (Balazs et al., 2012). AAV-based approaches could allow for continuous maternal mAb transfer throughout gestation and postpartum through human milk, potentially protecting both the mother and baby. Hyperimmune globulin represents an alternative strategy to provide HSV-specific Abs to the maternal–infant dyad, which may also protect from nHSV infection. Recently, this approach was employed to attempt to prevent congenital cytomegalovirus (CMV) infection via maternal treatment with CMV hyperimmune globulin. Ultimately, this strategy did not prevent congenital CMV, and treatment with hyperimmune globulin raised concerns over adverse obstetrical outcomes. These adverse outcomes were not statistically significant, but they were consistent with previous studies that also detected slightly higher risk in preterm birth, preeclampsia, and reduced fetal growth (Revello et al., 2014; Hughes et al., 2021). In contrast, the administration of mAbs during pregnancy has not been associated with these risks (Pham-Huy et al., 2021). Therefore, maternal mAb delivery may prove useful for other congenital and perinatal infections, especially for pathogens for which vaccination has failed or has not been attempted.

Infectious diseases account for approximately one-third of newborn deaths worldwide. Antenatal and perinatal infections of bacterial and viral etiology, including but not limited to Group B Streptococcus (GBS), CMV, and HSV, have devastating consequences. These infections result in significant neonatal death and life-long disability for the survivors (Whitley et al., 1991; Corey and Wald, 2009; Franciosi et al., 1973; Stagno et al., 1982; Stagno et al., 1986). Encouragingly, widespread screening and antenatal antibiotic use have significantly reduced the incidence of neonatal GBS, demonstrating that infection in early life can be circumvented if good therapies exist (Committee on Obstetrics Practice, 2020). Viral infections such as CMV and HSV remain a significant danger to neonates. While antiviral treatments have significant benefits in the reduction of mortality, they are unable to prevent long-term sequelae of nHSV. In the absence of additional interventions, such as vaccines or mAbs, consortiums and working groups are unlikely to recommend screening, leaving a gap in identifying affected pregnancies/newborns and failing to prevent significant morbidity and mortality even when diagnosed. Therefore, there is a great need to identify effective new therapeutic interventions for antenatal and perinatal infections as they have tremendous potential to save lives and improve long-term quality of life.

Materials and methods

Mouse procedures

C57BL/6 (B6) and B cell insufficient muMT (B6.129S2-*Ighm*^{tm1Cgn}/J) mice were purchased from The Jackson Laboratory (Kitamura et al., 1991). muMT mice were used in a subset of experiments to attribute protection to administered mAb, but the results were interchangeable with the B6 mice, which were therefore used for follow-up experiments. Blood collection was via cheek bleed from the mandibular vein with a 5-mm lancet for weanlings and adults or a 25 G needle for 1–2 wk-old pups. Animals <1 wk of age were euthanized prior to decapitation for blood collection. Blood samples were allowed to clot by stasis for ≥15 min and then spun at 2,000 × *g* for 10 min at 4°C and the supernatants were collected and stored at −20°C. mAbs were administered i.p. to pups in 20 µl. mAbs were administered i.p. to pregnant dams in volumes between 0.350 and 1 ml, to accommodate different mAb concentrations. For imaging studies, infected pups were injected i.p. with 20 µl of 15 mg/ml *D*-luciferin potassium salt (LUCK-100; GOLDBIO) and placed in an isoflurane chamber and moved into the Xenogen IVIS-200 (Caliper Life Sciences) with a warmed stage and continuous isoflurane. Pups were typically imaged 2 d postinfection and serially imaged every other day to monitor bioluminescence. Bioluminescence was determined by drawing a region of interest (ROI) of the same size per pup using the Living Image Software (Perkin Elmer). Background bioluminescence was determined by drawing a ROI on the stage in the absence of mouse pups. Endpoints for survival studies were defined as excessive morbidity (hunched, spasms, or paralysis) or >10% weight loss.

mAbs

CH42 and CH43 plasmids were kindly provided by Dr. Anthony Moody (Duke University, Durham, NC). When expressed in vitro, CH42 contained the Fc mutation known as AAA (S298A/E333A/K334A). This mutation has been shown to enhance binding to the activating human FcγRIIIa and decrease binding to activating FcγRIIa and inhibiting FcγRIIb, which overall enhances antibody-dependent cellular cytotoxicity (Shields et al., 2001; Liu et al., 2014). In murine model systems, similar mutations to (S298A/E333A/K334A) have enhanced FcγRIV binding, resulting in increased antibody-dependent cellular cytotoxicity (Liu et al., 2014). E317 is the original clone of the clinical drug product UB-621; its heavy and light chain variable sequences are derived from published amino acid sequences (Lai et al., 2010) and synthesized in-house. The heavy and light chain variable sequences were ordered as "gBlocks" (Integrated DNA Technologies) and cloned to an IgG1 heavy chain backbone and a κ light chain backbone. In-house expressed antibodies were made

through co-transfection of heavy and light chain plasmids in Expi293 HEK cells (Thermo Fisher Scientific) according to the manufacturer's instructions. 7 d after transfection, cultures were spun at 3,000 × *g* for 30 min to pellet the cells and the supernatants were filtered (0.22 µm). IgG was affinity purified using a custom-packed 5 ml protein A column with a retention time of 1 min (i.e., 5 ml/min) and eluted with 100 mM glycine, pH 3, which was immediately neutralized with 1 M Tris buffer, pH 8. The eluate was then concentrated to 2.5 ml for size exclusion chromatography on a HiPrep Sephacryl S-200 HR column using an AktaPure FPLC at a flow rate of 1 ml/min of sterile PBS. Fractions containing monomeric IgG were pooled and concentrated using spin columns (Amicon UFC903024) to ∼2 mg/ml of protein and either used within a week or aliquoted and frozen at −80°C for later use. HSV8 mAb was kindly provided by ZabBio, and UB-621, a clinical grade antibody preparation with the E317 gene sequence expressed in hamster ovary cells, was kindly provided by United Biopharma. Control IgG mAbs were made in-house and target HIV envelope glycoprotein.

Viral challenge

The WT viral strains used in this study were HSV-1 17syn$^+$ (Brown et al., 1973) and HSV-2 G (kindly provided by Dr. David Knipe; Ejercito et al., 1968). The bioluminescent luciferase-expressing recombinant virus HSV-1 17syn$^+$/Dlux was constructed as previously described (Luker et al., 2002). Viral stocks were prepared using Vero cells as previously described (Manivanh et al., 2017; Rader et al., 1993). Newborn pups were infected intranasally on day 1 or 2 postpartum with indicated amounts of HSV in a volume of 5 µl under isoflurane anesthesia. Pups were then monitored for survival and imaging. For survival studies, pups were challenged with 1×10^3 or 1×10^4 plaque-forming units (PFU) of HSV-1 (strain 17) and 3×10^2 PFU of HSV-2 (strain G) as indicated. Viral challenge doses were selected on the basis of prior investigations in which 50 or 100% of control litters succumbed to infection (Patel et al., 2019; Jiang et al., 2017). For imaging studies, pups were challenged with 1×10^5 PFU of HSV-1 17syn$^+$/Dlux, and this viral dose has been previously utilized to ascertain viral dissemination to the PNS, CNS, and viscera when infecting with WT virus and performing traditional viral plaque assays (Patel et al., 2019; Jiang et al., 2017). We, therefore, used this viral dose, which did not result in significant mortality, indicating that this strain is attenuated relative to the WT strain. Importantly, we observed replication in the viscera, CNS, and PNS, and continued to use this dose for our studies.

Whole body cryo-macrotome imaging procedures

Conjugation of mAb UB-621 was as previously described (Schneider et al., 2017). Briefly, 5 mg of mAb in 100 µl of PBS was incubated with 10 µl of filter-sterilized 1 M sodium bicarbonate and 1 µl of 10 mg/ml AF488 NHS-ester (Lumiprobe) for 1 h at room temperature and protected from light. Buffer exchange was carried out with Zeba spin columns (Thermo Fisher Scientific). B6 dams were bred for timed pregnancies, and on day 11 of gestation, a chlorophyll-free diet (ICN90460610; MP Biomedicals) was initiated to reduce autofluorescence. On day 16 of gestation, 5 mg AF488-labeled UB-621 was administered via tail-vein in a 100 µl volume, and 2 d later animals were sacrificed and prepared for cryo-imaging by OCT (Tissue-Tek) flooding and subsequent freezing at −20°C. The hyperspectral imaging whole body cryo-macrotome instrument has been described previously (Fitzgerald et al., 2020). Briefly, the system operates by automatically sectioning frozen specimens in a slice-and-image sequence, acquiring images of the specimen block after each section is removed. For this study, we acquired brightfield and AF488 fluorescence volumes of each animal at a resolution of 150 µm in the sectioning direction and ∼100 µm in the imaging plane. Hyperspectral fluorescence images were spectrally unmixed using known fluorophore and tissue spectral bases to isolate the AF488 signal in animal tissue. The acquired image stacks were then combined in an open-source software platform (Slicer 4.11) to generate high-resolution three-dimensional volumes of the brightfield and fluorophore distribution throughout whole-body animal models.

AAV production and procedure

AAVs encoding the heavy and light chain sequences of CH42, CH43, and E317, and control IgG (an IgG1 targeting the HIV envelope glycoprotein) mAbs with the same human IgG1 backbone were produced as previously described (Balazs et al., 2012). A single 40 µl injection of 1×10^{11} genome copies of AAV was administered into the gastrocnemius muscle of B6 mice as previously described (Balazs et al., 2012). Blood samples were obtained by cheek bleed to verify antibody expression.

Assessment of mAb expression and biodistribution

A magnetic bead-based assay (Brown et al., 2012) was used to measure antibody expression and biodistribution. Beads were conjugated to anti-human antigen-binding fragment (Fab) to capture mAbs of interest. Briefly, anti-human IgG F(ab')2 fragment (109-006-097; Jackson Immune Research) was conjugated to fluorescent microspheres (MagPlex-C Microspheres, Luminex Corp.) at a ratio of 6.5 µg protein/100 µl microspheres. Samples were diluted as indicated in mAb expression and biodistribution figures and then incubated with microspheres (500–750 beads/well) overnight at 4°C and washed in PBS with 1% BSA, 0.05% Tween-20, and 0.1% sodium azide. Anti-human IgG PE (2040-09; Southern Biotech) was incubated at 0.65 µg/ml for 45 min in PBS-TBN. The microspheres were washed and resuspended in 90 µl of sheath fluid (Luminex) and read using a Bio-plex array reader (FlexMap 3D, OR MAGPIX). The median fluorescence intensity of the PE signal was determined for each sample at indicated dilutions. For biodistribution assessment, the signal is reported as the fold increase in PE signal in treated pups relative to untreated controls.

Statistical analysis

Prism 8 GraphPad software was used for statistical tests unless otherwise described. For survival studies, HSV-specific mAbs were compared with isotype controls using the Log-rank Mantel–Cox test to determine P values. For BLI imaging studies, groups and time points were compared with each other via

two-way ANOVA, with Sidak's test for multiple comparisons to determine P values.

Study approval

Procedures were performed in accordance with Dartmouth's Center for Comparative Medicine and Research policies, and following approval by the institutional animal care and use committee.

Online supplemental material

Fig. S1 shows fluorescently labeled mAb signals measured by whole-body hyperspectral imaging. Fig. S2 shows BLI imaging of mouse pups and subsequent dissection to ascertain signal that includes the brain and trigeminal ganglia spread. Fig. S3 shows the biodistribution of maternally transferred VIP-derived mAbs and directly administered mAbs in pups. Table S1 summarizes the mAbs used in this study. Table S2 summarizes the survival experiments included in this publication. Video 1 shows fluorescently labeled mAb signal in fetal and maternal tissues via whole body hyperspectral imaging of a naïve and fluorescent-agent administered dam.

Acknowledgments

We gratefully appreciate Audra J. Charron for editing the manuscript and for thoughtful discussion. We acknowledge Alexey Khalenkov for the construction of HSV-1 17syn$^+$/Dlux, and appreciate Jennifer Fields with the Dartmouth Mouse Modeling Shared Resource (CA023108) for aid in animal studies. We also thank members of the Leib and Ackerman labs for materials and/or helpful discussion.

These studies were supported by National Institutes of Health grants (R21 AI147714-01 to D.A. Leib and M.E. Ackerman, and P01 AI098681 and R01 09083 to D.A. Leib). A.B. Balazs is supported by the National Institute on Drug Abuse (NIDA) Avenir New Innovator Award DP2DA040254, the MGH Transformative Scholars Program as well as funding from the Charles H. Hood Foundation. This independent research was supported by the Gilead Sciences Research Scholars Program in HIV.

Author contributions: I.M. Backes, S.C. Davis, A.B. Balazs, M.E. Ackerman, and D.A. Leib designed and analyzed the research. I.M. Backes, B.K. Byrd, M.D. Slein, C.D. Patel, S.A. Taylor, C.R. Garland, and S.W. MacDonald performed experiments, and/or made materials, engaged in discussion, and assisted with animal care and data analysis. I.M. Backes drafted the manuscript and prepared figures; M.E. Ackerman and D.A. Leib edited the manuscript and figure legends; and other authors contributed comments and edits.

Disclosures: I.M. Backes reported a patent to WO2020077119A1 issued and a patent to 029511-8082 pending; and United Biopharma provided mAb UB-621 for experiments. ZabBio provided mAb HSV8. C.D. Patel reported a patent to US20210340223A1 pending. A.B. Balazs reported a patent to US20120232133A1 issued. S.C. Davis reported personal fees from GV LLP (formerly Google Ventures) outside the submitted work. He is expanding upon the relationship with GV LLP: There is no connection between my relationship with this entity and the work being submitted. He is disclosing this because his role with the entity generally involves investing in the biomedical space. M.E. Ackerman reported grants from NIH, and non-financial support from Zabb and United Biopharma during the conduct of the study; and grants from NIH and the Bill and Melinda Gates Foundation outside the submitted work; in addition, M.E. Ackerman had a patent to US20210340223A1 pending. D.A. Leib reported a patent to 62/744,325 pending. No other disclosures were reported.

Submitted: 18 January 2022
Revised: 29 March 2022
Accepted: 1 September 2022

References

Balazs, A.B., J.D. Bloom, C.M. Hong, D.S. Rao, and D. Baltimore. 2013. Broad protection against influenza infection by vectored immunoprophylaxis in mice. *Nat. Biotechnol.* 31:647–652. https://doi.org/10.1038/nbt.2618

Balazs, A.B., J. Chen, C.M. Hong, D.S. Rao, L. Yang, and D. Baltimore. 2011. Antibody-based protection against HIV infection by vectored immunoprophylaxis. *Nature*. 481:81–84. https://doi.org/10.1038/nature10660

Balazs, A.B., Y. Ouyang, C.M. Hong, J. Chen, S.M. Nguyen, D.S. Rao, D.S. An, and D. Baltimore. 2014. Vectored immunoprophylaxis protects humanized mice from mucosal HIV transmission. *Nat. Med.* 20:296–300. https://doi.org/10.1038/nm.3471

Belshe, R.B., P.A. Leone, D.I. Bernstein, A. Wald, M.J. Levin, J.T. Stapleton, I. Gorfinkel, R.L.A. Morrow, M.G. Ewell, A. Stokes-Riner, et al. 2012. Efficacy results of a trial of a herpes simplex vaccine. *N. Engl. J. Med.* 366:34–43. https://doi.org/10.1056/NEJMoa1103151

Booth, B.J., B. Ramakrishnan, K. Narayan, A.M. Wollacott, G.J. Babcock, Z. Shriver, and K. Viswanathan. 2018. Extending human IgG half-life using structure-guided design. *mAbs*. 10:1098–1110. https://doi.org/10.1080/19420862.2018.1490119

Brown, E.P., A.F. Licht, A.S. Dugast, I. Choi, C. Bailey-Kellogg, G. Alter, and M.E. Ackerman. 2012. High-throughput, multiplexed IgG subclassing of antigen-specific antibodies from clinical samples. *J. Immunol. Methods*. 386:117–123. https://doi.org/10.1016/j.jim.2012.09.007

Brown, S.M., D.A. Ritchie, and J.H. Subak-Sharpe. 1973. Genetic studies with herpes simplex virus type 1. The isolation of temperature-sensitive mutants, their arrangement into complementation groups and recombination analysis leading to a linkage map. *J. Gen. Virol.* 18:329–346. https://doi.org/10.1099/0022-1317-18-3-329

Brown, Z.A., J. Benedetti, R. Ashley, S. Burchett, S. Selke, S. Berry, L.A. Vontver, and L. Corey. 1991. Neonatal herpes simplex virus infection in relation to asymptomatic maternal infection at the time of labor. *N. Engl. J. Med.* 324:1247–1252. https://doi.org/10.1056/NEJM199105023241804

Brown, Z.A., S. Selke, J. Zeh, J. Kopelman, A. Maslow, R.L. Ashley, D.H. Watts, S. Berry, M. Herd, and L. Corey. 1997. The acquisition of herpes simplex virus during pregnancy. *N. Engl. J. Med.* 337:509–515. https://doi.org/10.1056/NEJM199708213370801

Brown, Z.A., A. Wald, R.A. Morrow, S. Selke, J. Zeh, and L. Corey. 2003. Effect of serologic status and cesarean delivery on transmission rates of herpes simplex virus from mother to infant. *JAMA*. 289:203–209. https://doi.org/10.1001/jama.289.2.203

Bulcha, J.T., Y. Wang, H. Ma, P.W.L. Tai, and G. Gao. 2021. Viral vector platforms within the gene therapy landscape. *Signal Transduct. Targeted Ther.* 6:53. https://doi.org/10.1038/s41392-021-00487-6

Burioni, R., R.A. Williamson, P.P. Sanna, F.E. Bloom, and D.R. Burton. 1994. Recombinant human Fab to glycoprotein D neutralizes infectivity and prevents cell-to-cell transmission of herpes simplex viruses 1 and 2 in vitro. *Proc. Natl. Acad. Sci. USA*. 91:355–359. https://doi.org/10.1073/pnas.91.1.355

Casazza, J.P., E.M. Cale, S. Narpala, G.V. Yamshchikov, E.E. Coates, C.S. Hendel, L. Novik, L.A. Holman, A.T. Widge, P. Apte, et al. 2022. Safety and tolerability of AAV8 delivery of a broadly neutralizing antibody in adults living with HIV: A phase 1, dose-escalation trial. *Nat. Med.* 28:1022–1030. https://doi.org/10.1038/s41591-022-01762-x

Clementi, N., E. Criscuolo, F. Cappelletti, R. Burioni, M. Clementi, and N. Mancini. 2016. Novel therapeutic investigational strategies to treat severe and disseminated HSV infections suggested by a deeper understanding of in vitro virus entry processes. *Drug Disc. Today*. 21: 682–691. https://doi.org/10.1016/j.drudis.2016.03.003

Committee on Obstetrics Practice. 2020. Prevention of group B streptococcal early-onset disease in newborns: ACOG committee opinion, number 797. *Obstet. Gynecol.* 135:e51–e72. https://doi.org/10.1097/AOG.0000000000003668

Corey, L., A.G. Langenberg, R. Ashley, R.E. Sekulovich, A.E. Izu, J.M. Douglas Jr, H.H. Handsfield, T. Warren, L. Marr, S. Tyring, et al. 1999. Recombinant glycoprotein vaccine for the prevention of genital HSV-2 infection: Two randomized controlled trials. Chiron HSV Vaccine Study Group. *JAMA*. 282:331–340. https://doi.org/10.1001/jama.282.4.331

Corey, L., and A. Wald. 2009. Maternal and neonatal herpes simplex virus infections. *N. Engl. J. Med.* 361:1376–1385. https://doi.org/10.1056/NEJMra0807633

Cunningham, C.K., E.J. McFarland, R.L. Morrison, E.V. Capparelli, J.T. Safrit, L.M. Mofenson, B. Mathieson, M.E. Valentine, C. Perlowski, B. Smith, et al. 2020. Safety, tolerability, and pharmacokinetics of the broadly neutralizing human immunodeficiency virus (HIV)-1 monoclonal antibody VRC01 in HIV-exposed newborn infants. *J. Infect. Dis.* 222: 628–636. https://doi.org/10.1093/infdis/jiz532

De Logu, A., R.A. Williamson, R. Rozenshteyn, F. Ramiro-Ibañez, C.D. Simpson, D.R. Burton, and P.P. Sanna. 1998. Characterization of a type-common human recombinant monoclonal antibody to herpes simplex virus with high therapeutic potential. *J. Clin. Microbiol.* 36:3198–3204. https://doi.org/10.1128/JCM.36.11.3198-3204.1998

Deal, C., A.B. Balazs, D.A. Espinosa, F. Zavala, D. Baltimore, and G. Ketner. 2014. Vectored antibody gene delivery protects against *Plasmodium falciparum* sporozoite challenge in mice. *Proc. Natl. Acad. Sci. USA*. 111: 12528–12532. https://doi.org/10.1073/pnas.1407362111

Dix, R.D., L. Pereira, and J.R. Baringer. 1981. Use of monoclonal antibody directed against herpes simplex virus glycoproteins to protect mice against acute virus-induced neurological disease. *Infect. Immun.* 34: 192–199. https://doi.org/10.1128/iai.34.1.192-199.1981

Ejercito, P.M., E.D. Kieff, and B. Roizman. 1968. Characterization of herpes simplex virus strains differing in their effects on social behaviour of infected cells. *J. Gen. Virol.* 2:357–364. https://doi.org/10.1099/0022-1317-2-3-357

Evans, I.A.C., and C.A. Jones. 2002. Maternal immunization with a herpes simplex virus type 2 replication-defective virus reduces visceral dissemination but not lethal encephalitis in newborn mice after oral challenge. *J. Infect. Dis.* 185:1550–1560. https://doi.org/10.1086/340572

Fitzgerald, J.E., B.K. Byrd, R.A. Patil, R.R. Strawbridge, S.C. Davis, C. Bellini, and M. Niedre. 2020. Heterogeneity of circulating tumor cell dissemination and lung metastases in a subcutaneous Lewis lung carcinoma model. *Biomed. Opti. Express*. 11:3633–3647. https://doi.org/10.1364/BOE.395289

Franciosi, R.A., J.D. Knostman, and R.A. Zimmerman. 1973. Group B streptococcal neonatal and infant infections. *J. Pediatr.* 82:707–718. https://doi.org/10.1016/S0022-3476(73)80604-3

Gaudet, D., E.S. Stroes, J. Méthot, D. Brisson, K. Tremblay, S.J. Bernelot Moens, G. Iotti, I. Rastelletti, D. Ardigo, D. Corzo, et al. 2016. Long-term retrospective analysis of gene therapy with alipogene tiparvovec and its effect on lipoprotein lipase deficiency-induced pancreatitis. *Hum. Gene Ther.* 27:916–925. https://doi.org/10.1089/hum.2015.158

Hook, L.M., T.M. Cairns, S. Awasthi, B.D. Brooks, N.T. Ditto, R.J. Eisenberg, G.H. Cohen, and H.M. Friedman. 2018. Vaccine-induced antibodies to herpes simplex virus glycoprotein D epitopes involved in virus entry and cell-to-cell spread correlate with protection against genital disease in Guinea pigs. *PLoS Pathog.* 14:e1007095. https://doi.org/10.1371/journal.ppat.1007095

Hughes, B.L., R.G. Clifton, D.J. Rouse, G.R. Saade, M.J. Dinsmoor, U.M. Reddy, R. Pass, D. Allard, G. Mallett, L.M. Fette, et al. 2021. A trial of hyperimmune globulin to prevent congenital cytomegalovirus infection. *N. Engl. J. Med.* 385:436–444. https://doi.org/10.1056/NEJMoa1913569

Jiang, Y., C.D. Patel, R. Manivanh, B. North, I.M. Backes, D.A. Posner, F. Gilli, A.R. Pachner, L.N. Nguyen, and D.A. Leib. 2017. Maternal antiviral immunoglobulin accumulates in neural tissue of neonates to prevent HSV neurological disease. *mBio*. 8:e00678-17. https://doi.org/10.1128/mBio.00678-17

Jong, Y.P., M. Dorner, M.C. Mommersteeg, J.W. Xiao, A.B. Balazs, J.B. Robbins, B.Y. Winer, S. Gerges, K. Vega, R.N. Labitt, et al. 2014. Broadly neutralizing antibodies abrogate established hepatitis C virus infection. *Sci. Trans. Med.* 6:254ra129. https://doi.org/10.1126/scitranslmed.3009512

Kao, C.M., J. Goymer, L.N. Loh, A. Mahant, C.B. Aschner, and B.C. Herold. 2020. Murine model of maternal immunization demonstrates protective role for antibodies that mediate antibody-dependent cellular cytotoxicity in protecting neonates from herpes simplex virus type 1 and type 2. *J. Infect. Dis.* 221:729–738. https://doi.org/10.1093/infdis/jiz521

Kim, J., S. Mohanty, L.P. Ganesan, K. Hua, D. Jarjoura, W.L. Hayton, J.M. Robinson, and C.L. Anderson. 2009. FcRn in the yolk sac endoderm of mouse is required for IgG transport to fetus. *J. Immunol.* 182:2583–2589. https://doi.org/10.4049/jimmunol.0803247

Kimberlin, D.M. 2007. Immunotherapy of HSV infections – antibody delivery. In *Human Herpesviruses: Biology, Therapy, and Immunoprophylaxis*. A. Arvin, G. Campadelli-Fiume, E. Mocarski, P.S. Moore, B. Roizman, R. Whitley, and K. Yamanishi, editors. Cambridge University Press, Cambridge.

Kitamura, D., J. Roes, R. Kühn, and K. Rajewsky. 1991. A B cell-deficient mouse by targeted disruption of the membrane exon of the immunoglobulin mu chain gene. *Nature*. 350:423–426. https://doi.org/10.1038/350423a0

Kohl, S. 1991. Role of antibody-dependent cellular cytotoxicity in neonatal infection with herpes simplex virus. *Rev. Infect. Dis.* 13:S950–S952. https://doi.org/10.1093/clind/13.Supplement_11.S950

Kohl, S., and L.S. Loo. 1980. Ontogeny of murine cellular cytotoxicity to herpes simplex virus-infected cells. *Infect. Immun.* 30:847–850. https://doi.org/10.1128/iai.30.3.847-850.1980

Kohl, S., N.C. Strynadka, R.S. Hodges, and L. Pereira. 1990. Analysis of the role of antibody-dependent cellular cytotoxic antibody activity in murine neonatal herpes simplex virus infection with antibodies to synthetic peptides of glycoprotein D and monoclonal antibodies to glycoprotein B. *J. Clin. Invest.* 86:273–278. https://doi.org/10.1172/JCI114695

Kohl, S., M.S. West, C.G. Prober, W.M. Sullender, L.S. Loo, and A.M. Arvin. 1989. Neonatal antibody-dependent cellular cytotoxic antibody levels are associated with the clinical presentation of neonatal herpes simplex virus infection. *J. Infect. Dis.* 160:770–776. https://doi.org/10.1093/infdis/160.5.770

Kopp, S.J., G. Banisadr, K. Glajch, U.E. Maurer, K. Grünewald, R.J. Miller, P. Osten, and P.G. Spear. 2009. Infection of neurons and encephalitis after intracranial inoculation of herpes simplex virus requires the entry receptor nectin-1. *Proc. Natl. Acad. Sci. USA*. 106:17916–17920. https://doi.org/10.1073/pnas.0908892106

Kopp, S.J., A.H. Karaba, L.K. Cohen, G. Banisadr, R.J. Miller, and W.J. Muller. 2013. Pathogenesis of neonatal herpes simplex 2 disease in a mouse model is dependent on entry receptor expression and route of inoculation. *J. Virol.* 87:474–481. https://doi.org/10.1128/JVI.01849-12

Kopp, S.J., H.R. Ranaivo, D.R. Wilcox, A.H. Karaba, M.S. Wainwright, and W.J. Muller. 2014. Herpes simplex virus serotype and entry receptor availability alter CNS disease in a mouse model of neonatal HSV. *Pediatr. Res.* 76:528–534. https://doi.org/10.1038/pr.2014.135

Krawczyk, A., M.A.E. Arndt, L. Grosse-Hovest, W. Weichert, B. Giebel, U. Dittmer, H. Hengel, D. Jager, K.E. Schneweis, A.M. Eis-Hubinger, et al. 2013. Overcoming drug-resistant herpes simplex virus (HSV) infection by a humanized antibody. *Proc. Natl. Acad. Sci. USA*. 110:6760–6765. https://doi.org/10.1073/pnas.1220019110

Lai, J.-S., and W.-E. Chan. Development Center for Biotechnology, LLC, assignee. 2013. Anti-herpes simplex virus antibodies and methods of use thereof. United States patent 8,431,118B2, filed January 5, 2009, and issued April 30, 2013.

Lai, J.-S., Y.-S. Lin, and W.-E. Chan. Development Center for Biotechnology, LLC, assignee. 2010. Anti-herpes simplex virus antibodies. World Intellectual Property Organization patent WO/2010/087813A1, filed January 5, 2009, and issued August 5, 2010.

Lee, C.-C., L.-L. Lin, W.-E. Chan, T.-P. Ko, J.-S. Lai, and A.H.-J. Wang. 2013. Structural basis for the antibody neutralization of *Herpes simplex virus*. *Acta Crystallogr. D Biol. Crystallogr.* 69:1935–1945. https://doi.org/10.1107/S0907444913016776

Liu, Z., K. Gunasekaran, W. Wang, V. Razinkov, L. Sekirov, E. Leng, H. Sweet, I. Foltz, M. Howard, A.-M. Rousseau, et al. 2014. Asymmetrical Fc engineering greatly enhances antibody-dependent cellular cytotoxicity (ADCC) effector function and stability of the modified antibodies. *J. Biol. Chem.* 289:3571–3590. https://doi.org/10.1074/jbc.M113.513366

Looker, K.J., A.S. Magaret, M.T. May, K.M.E. Turner, P. Vickerman, L.M. Newman, and S.L. Gottlieb. 2017. First estimates of the global and regional incidence of neonatal herpes infection. *Lancet Glob. Health*. 5: e300–e309. https://doi.org/10.1016/S2214-109X(16)30362-X

Luker, G.D., J.P. Bardill, J.L. Prior, C.M. Pica, D. Piwnica-Worms, and D.A. Leib. 2002. Noninvasive bioluminescence imaging of herpes simplex virus type 1 infection and therapy in living mice. *J. Virol.* 76:12149–12161. https://doi.org/10.1128/JVI.76.23.12149-12161.2002

Mahant, S., M. Hall, A.C. Schondelmeyer, J.G. Berry, D.W. Kimberlin, S.S. Shah, and Pediatric Research in Inpatient Settings Network and the Collaborative Antiviral Study Group. 2019. Neonatal herpes simplex virus infection among medicaid-enrolled children: 2009-2015. *Pediatrics*. 143:e20183233. doi:https://doi.org/10.1542/peds.2018-3233

Manivanh, R., J. Mehrbach, D.M. Knipe, and D.A. Leib. 2017. Role of herpes simplex virus 1 γ34.5 in the regulation of IRF3 signaling. *J. Virol.* 91: e01156-17. https://doi.org/10.1128/JVI.01156-17

McFarland, E.J., C.K. Cunningham, P. Muresan, E.V. Capparelli, C. Perlowski, P. Morgan, B. Smith, R. Hazra, L. Purdue, P.A. Harding, et al. 2021. Safety, tolerability, and pharmacokinetics of a long-acting broadly neutralizing human immunodeficiency virus type 1 (HIV-1) monoclonal antibody VRC01LS in HIV-1-Exposed newborn infants. *J. Infect. Dis.* 224: 1916. https://doi.org/10.1093/infdis/jiab229

McKendall, R.R., T. Klassen, and J.R. Baringer. 1979. Host defenses in herpes simplex infections of the nervous system: Effect of antibody on disease and viral spread. *Infect. Immun.* 23:305–311. https://doi.org/10.1128/iai.23.2.305-311.1979

Oakes, J.E. 1975. Invasion of the central nervous system by herpes simplex virus type 1 after subcutaneous inoculation of immunosuppressed mice. *J. Infect. Dis.* 131:51–57. https://doi.org/10.1093/infdis/131.1.51

Patel, C.D. 2020. Harnessing maternal humoral immunity to prevent neonatal herpes neurological sequela. Dartmouth College, United States, New Hampshire. 188 pp.

Patel, C.D., I.M. Backes, S.A. Taylor, Y. Jiang, A. Marchant, J.M. Pesola, D.M. Coen, D.M. Knipe, M.E. Ackerman, and D.A. Leib. 2019. Maternal immunization confers protection against neonatal herpes simplex mortality and behavioral morbidity. *Sci. Transl. Med.* 11:eaau6039. https://doi.org/10.1126/scitranslmed.aau6039

Patel, C.D., S.A. Taylor, J. Mehrbach, S. Awasthi, H.M. Friedman, and D.A. Leib. 2020. Trivalent glycoprotein subunit vaccine prevents neonatal herpes simplex virus mortality and morbidity. *J. Virol.* 94:e021633-19. https://doi.org/10.1128/JVI.02163-19

Pham-Huy, A., K.A. Top, C. Constantinescu, C.H. Seow, and D. El-Chaâr. 2021. The use and impact of monoclonal antibody biologics during pregnancy. *CMAJ*. 193:E1129–E1136. https://doi.org/10.1503/cmaj.202391

Politch, J.A., S. Cu-Uvin, T.R. Moench, K.T. Tashima, J.G. Marathe, K.M. Guthrie, H. Cabral, T. Nyhuis, M. Brennan, L. Zeitlin, et al. 2021. Safety, acceptability, and pharmacokinetics of a monoclonal antibody-based vaginal multipurpose prevention film (MB66): A phase I randomized trial. *PLoS Med.* 18:e1003495. https://doi.org/10.1371/journal.pmed.1003495

Priddy, F.H., D.J.M. Lewis, H.C. Gelderblom, H. Hassanin, C. Streatfield, C. LaBranche, J. Hare, J.H. Cox, L. Dally, D. Bendel, et al. 2019. Adeno-associated virus vectored immunoprophylaxis to prevent HIV in healthy adults: A phase 1 randomised controlled trial. *Lancet HIV*. 6: e230–e239. https://doi.org/10.1016/S2352-3018(19)30003-7

Rader, K.A., C.E. Ackland-Berglund, J.K. Miller, J.S. Pepose, and D.A. Leib. 1993. In vivo characterization of site-directed mutations in the promoter of the herpes simplex virus type 1 latency-associated transcripts. *J. Gen. Virol.* 74:1859–1869. https://doi.org/10.1099/0022-1317-74-9-1859

Revello, M.G., T. Lazzarotto, B. Guerra, A. Spinillo, E. Ferrazzi, A. Kustermann, S. Guaschino, P. Vergani, T. Todros, T. Frusca, et al. 2014. A randomized trial of hyperimmune globulin to prevent congenital cytomegalovirus. *N. Engl. J. Med.* 370:1316–1326. https://doi.org/10.1056/NEJMoa1310214

Sáez-Llorens, X., E. Castaño, D. Null, J. Steichen, P.J. Sánchez, O. Ramilo, F.H. Top, and E. Connor. 1998. Safety and pharmacokinetics of an intramuscular humanized monoclonal antibody to respiratory syncytial virus in premature infants and infants with bronchopulmonary dysplasia. The MEDI-493 Study Group. *Pediatr. Infect. Dis. J.* 17:787–791. https://doi.org/10.1097/00006454-199809000-00007

Sanna, P.P., A. De logu, R.A. Williamson, Y.-L. Hom, S.E. Straus, F.E. Bloom, and D.R. Burton. 1996. Protection of nude mice by passive immunization with a type-common human recombinant monoclonal antibody against HSV. *Virology*. 215:101–106. https://doi.org/10.1006/viro.1996.0011

Schneider, J.R., A.M. Carias, A.R. Bastian, G.C. Cianci, P.F. Kiser, R.S. Veazey, and T.J. Hope. 2017. Long-term direct visualization of passively transferred fluorophore-conjugated antibodies. *J. Immunol. Methods*. 450: 66–72. https://doi.org/10.1016/j.jim.2017.07.009

Shah, S.S., P.L. Aronson, Z. Mohamad, and S.A. Lorch. 2011. Delayed acyclovir therapy and death among neonates with herpes simplex virus infection. *Pediatrics*. 128:1153–1160. https://doi.org/10.1542/peds.2011-0177

Sheffield, J.S., J.B. Hill, L.M. Hollier, V.R. Laibl, S.W. Roberts, P.J. Sanchez, and G.D. Wendel Jr. 2006. Valacyclovir prophylaxis to prevent recurrent herpes at delivery: A randomized clinical trial. *Obstet. Gynecol.* 108: 141–147. https://doi.org/10.1097/01.AOG.0000219749.96274.15

Shields, R.L., A.K. Namenuk, K. Hong, Y.G. Meng, J. Rae, J. Briggs, D. Xie, J. Lai, A. Stadlen, B. Li, et al. 2001. High resolution mapping of the binding site on human IgG1 for FcγRI, FcγRII, FcγRIII, and FcRn and design of IgG1 variants with improved binding to the FcγR. *J. Biol. Chem.* 276: 6591–6604. https://doi.org/10.1074/jbc.M009483200

Slutsker, J.S., and J.A. Schillinger. 2021. Assessing the burden of infant deaths due to herpes simplex virus, human immunodeficiency virus, and congenital syphilis: United States, 1995 to 2017. *Sex. Transm. Dis.* 48: S4–S10. https://doi.org/10.1097/OLQ.0000000000001458

Soter, J.A., E.P.M. LaRochelle, B.K. Byrd, I.I. Tendler, J.R. Gunn, B. Meng, R.R. Strawbridge, D.J. Wirth, S.C. Davis, D.J. Gladstone, et al. 2020. Tracking tumor radiotherapy response in vivo with Cherenkov-excited luminescence ink imaging. *Phys. Med. Biol.* 65:095004. https://doi.org/10.1088/1361-6560/ab7d16

Stagno, S., R.F. Pass, G. Cloud, W.J. Britt, R.E. Henderson, P.D. Walton, D.A. Veren, F. Page, and C.A. Alford. 1986. Primary cytomegalovirus infection in pregnancy. Incidence, transmission to fetus, and clinical outcome. *JAMA*. 256:1904–1908

Stagno, S., R.F. Pass, M.E. Dworsky, and C.A. Alford. 1982. Maternal cytomegalovirus infection and perinatal transmission. *Clin. Obstet. Gynecol.* 25:563–576. https://doi.org/10.1097/00003081-198209000-00014

Stannard, L.M., A.O. Fuller, and P.G. Spear. 1987 Spear1987. Herpes simplex virus glycoproteins associated with different morphological entities projecting from the virion envelope. *J. Gen. Virol.* 68:715–725. https://doi.org/10.1099/0022-1317-68-3-715

Subramanian, K.N., L.E. Weisman, T. Rhodes, R. Ariagno, P.J. Sánchez, J. Steichen, L.B. Givner, T.L. Jennings, F.H. Top, D. Carlin, and E. Connor. 1998. Safety, tolerance and pharmacokinetics of a humanized monoclonal antibody to respiratory syncytial virus in premature infants and infants with bronchopulmonary dysplasia. MEDI-493 Study Group. *Pediatr. Infect. Dis. J.* 17:110–115. https://doi.org/10.1097/00006454-199802000-00006

Summers, B.C., T.P. Margolis, and D.A. Leib. 2001. Herpes simplex virus type 1 corneal infection results in periocular disease by zosteriform spread. *J. Virol.* 75:5069–5075. https://doi.org/10.1128/JVI.75.11.5069-5075.2001

Wang, K., G.D. Tomaras, S. Jegaskanda, M.A. Moody, H.-X. Liao, K.N. Goodman, P.W. Berman, S. Rerks-Ngarm, P. Pitisuttithum, S. Nitayapan, et al. 2017. Monoclonal antibodies, derived from humans vaccinated with the RV144 HIV vaccine containing the HVEM binding domain of herpes simplex virus (HSV) glycoprotein D, neutralize HSV infection, mediate antibody-dependent cellular cytotoxicity, and protect mice from ocular challenge with HSV-1. *J. Virol.* 91:e00411-17. https://doi.org/10.1128/JVI.00411-17

Whitley, R., A. Arvin, C. Prober, L. Corey, S. Burchett, S. Plotkin, S. Starr, R. Jacobs, D. Powell, and A. Nahmias. 1991. Predictors of morbidity and mortality in neonates with herpes simplex virus infections. The national institute of allergy and infectious diseases collaborative antiviral study group. *N. Engl. J. Med.* 324:450–454. https://doi.org/10.1056/NEJM199102143240704

Whitley, R.J., A.J. Nahmias, A.M. Visintine, C.L. Fleming, C.A. Alford, A. Yeager, A. Arvin, R. Haynes, M. Hilty, and J. Luby. 1980. The natural history of herpes simplex virus infection of mother and newborn. *Pediatrics*. 66:489–494. https://doi.org/10.1542/peds.66.4.489

Williams, E.J., N.D. Embleton, J.E. Clark, M. Bythell, M.P. Ward Platt, and J.E. Berrington. 2013. Viral infections: Contributions to late fetal death, stillbirth, and infant death. *J. Pediatr.* 163:424–428. https://doi.org/10.1016/j.jpeds.2013.02.004

Yeager, A.S., A.M. Arvin, L.J. Urbani, and J.A. Kemp. 1981. Relationship of antibody to outcome in neonatal herpes simplex virus infections. *Obstet. Gynecol. Surv.* 36:191–192. https://doi.org/10.1097/00006254-198104000-00012

Zalevsky, J., A.K. Chamberlain, H.M. Horton, S. Karki, I.W.L. Leung, T.J. Sproule, G.A. Lazar, D.C. Roopenian, and J.R. Desjarlais. 2010. Enhanced antibody half-life improves in vivo activity. *Nat. Biotechnol.* 28:157–159. https://doi.org/10.1038/nbt.1601

Zawatzky, R., H. Engler, and H. Kirchner. 1982. Experimental infection of inbred mice with herpes simplex virus. III. Comparison between newborn and adult C57BL/6 mice. *J. Gen. Virol.* 60:25–29. https://doi.org/10.1099/0022-1317-60-1-25

Supplemental material

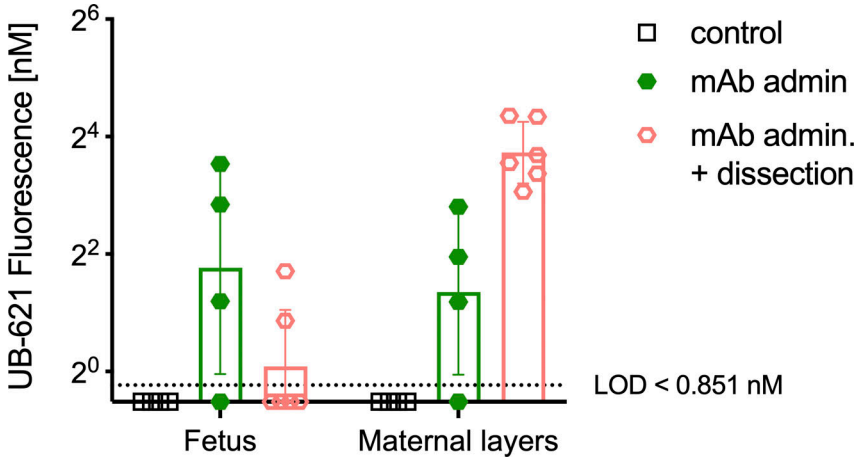

Figure S1. **Fluorescently labeled mAb signals in fetal and maternal tissues measured by whole-body hyperspectral imaging.** To assess maternally administered Ab biodistribution, conjugated Ab was administered IV on day 15 or 16 of gestation, then 2–3 d later tissues were prepared for imaging with the whole body cryo-macrotome, mAb admin (dam n = 1, pup n = 4), mAb admin. + dissection (dam n = 1, pup n = 6). Control background fluorescence was determined in a pregnant dam not injected with conjugated Ab (dam n = 1, pup n = 4). Each dot represents the average intensity value of all voxels for a single animal, bar represents the full cohort's geometric mean fluorescence intensity value, and the error is reported as geometric standard deviation (n = 4–6 per cohort).

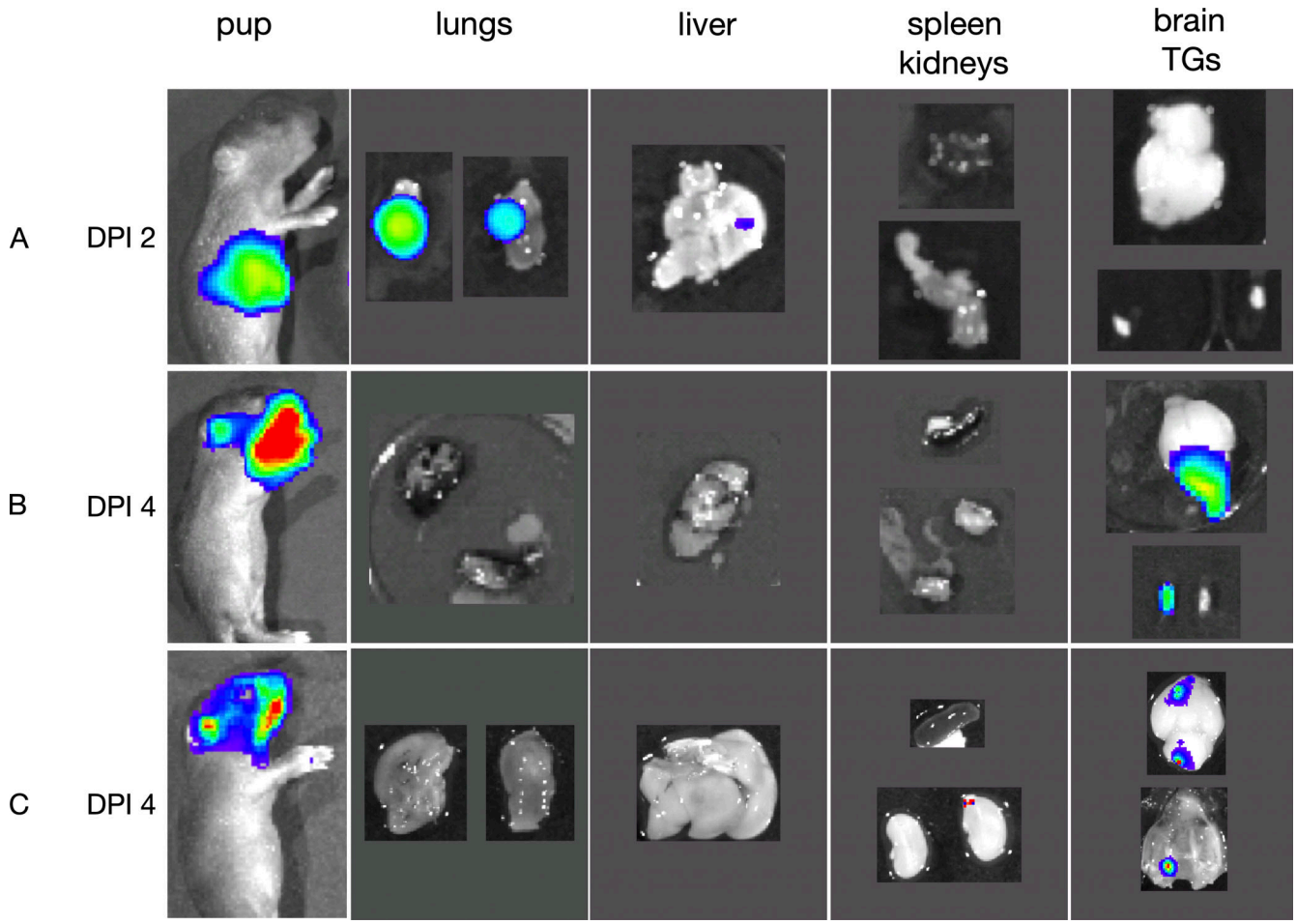

Figure S2. **Rostral bioluminescence derives from the brain and trigeminal ganglia.** Pups (n = 3) were challenged with 1 × 10^5 PFU of luciferase-expressing HSV-1, then imaged following i.p. administration of 20 ul of luciferin (15 mg/ml). **(A)** Bioluminescence of pup imaged, and immediately sacrificed and dissected on DPI 2. **(B and C)** Bioluminescence of pups imaged, and immediately sacrificed and dissected on DPI 4. DPI, days postinfection.

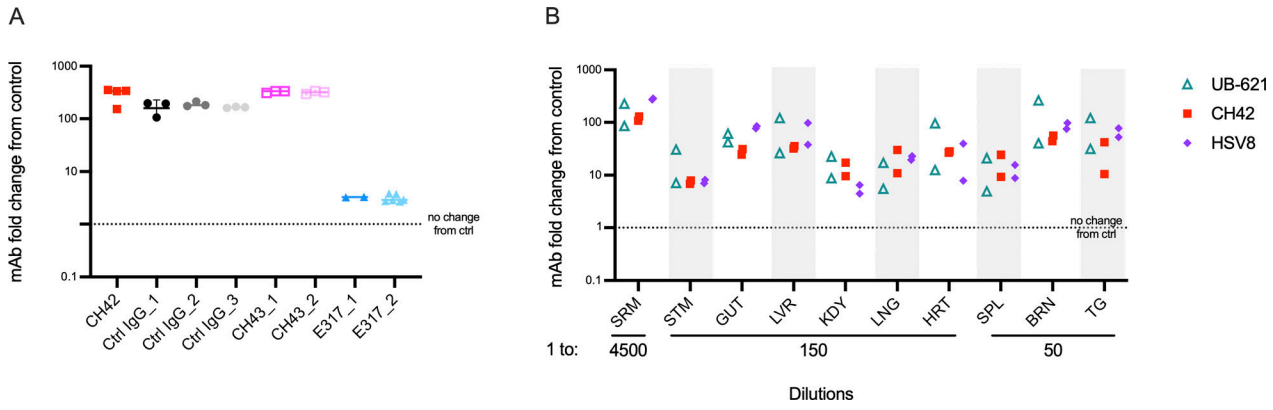

Figure S3. **Distribution of maternally transferred VIP-derived mAbs and directly administered mAbs in pups.** Magnetic bead-based assays were used to detect hIgG transfer and biodistribution. **(A)** Detection of in vivo expressed huIgG in the serum (diluted 1–300) of 2-d-old progeny of AAV-administered dams, each column represents an individual AAV-transduced dam, and each symbol within the column a mouse pup, the line represents the median value. CH42 (dam n = 1, pup n = 4); Ctrl IgG (dam n = 3, pup n = 9); CH43 (dam n = 2, pup n = 6); E317 (dam n = 2, pup n = 6). **(B)** Biodistribution of huIgG of pups 48 h after intraperitoneal administration of mAbs UB-621 (pup n = 2), CH42 (pup n = 2), HSV8 (pup n = 2). Each symbol represents a mouse pup. Signal is reported as the fold increase in huIgG in treated pups relative to untreated controls. Serum (SRM), stomach (STM), lung (LNG), liver (LVR), heart (HRT), kidney (KDY), spleen (SPL), trigeminal ganglia (TG), brain (BRN).

Video 1. **Fluorescently labeled mAb signal in fetal and maternal tissues via whole body hyperspectral imaging.** Experimental set up as described in Fig. S1. Left video shows a naïve control dam that did not receive fluorescent mAb, right video shows dam administered AF488-conjugated UB-621. Playback speed is 10 frames/s. Please note that this is not live imaging so the playback speed is not related to time during a longitudinally assessed process.

Provided online are Table S1 and Table S2. Table S1 provides a summary of the mAbs used in this study. Table S2 provides a summary of survival experiments performed in this study.